Comparative Biochemistry and Physiology, Part B 168 (2014) 1–11

Contents lists available at ScienceDirect

Comparative Biochemistry and Physiology, Part B

journal homepage: www.elsevier.com/locate/cbpb

Molecular diversity and body distribution of saponins in the sea star *Asterias rubens* by mass spectrometry

Marie Demeyer [a,b], Julien De Winter [a], Guillaume Caulier [b], Igor Eeckhaut [b], Patrick Flammang [b,*], Pascal Gerbaux [a,*]

[a] Mass Spectrometry Research Group, Interdisciplinary Center for Mass Spectrometry, University of Mons — UMONS, 23 Place du Parc, B-7000 Mons, Belgium
[b] Biology of Marine Organisms and Biomimetics, University of Mons — UMONS, 23 Place du Parc, B-7000 Mons, Belgium

ARTICLE INFO

Article history:
Received 29 August 2013
Received in revised form 21 October 2013
Accepted 21 October 2013
Available online 29 October 2013

Keywords:
Echinoderms
Saponins
Mass spectrometry
Structure elucidation
Natural products
LC-MS

ABSTRACT

Saponins are natural molecules that the common sea star *Asterias rubens* produces in the form of steroid glycosides bearing a sulfate group attached on the aglycone part. In order to highlight the inter-organ and inter-individual variability, the saponin contents of five distinct body components, namely the aboral body wall, the oral body wall, the stomach, the pyloric caeca and the gonads, from different individuals were separately analyzed by mass spectrometry. MALDI–ToF experiments were selected as the primary tool for a rapid screening of the saponin mixtures, whereas LC–MS and LC–MS/MS techniques were used to achieve chromatographic separation of isomers. First of all, our analyses demonstrated that the diversity of saponins is higher than previously reported. Indeed, nine new congeners were observed in addition to the 17 saponins already described in this species. On the basis of all the collected MS/MS data, we also identified collision-induced key-fragmentations that could be used to reconstruct the molecular structure of both known and unknown saponin ions. Secondly, the comparison of the saponin contents from the five different body components revealed that each organ is characterized by a specific mixture of saponins and that between animals there are also qualitative and quantitative variability of the saponin contents which could be linked to the sex or to the collecting season. Therefore, the observed high variability unambiguously confirms that saponins probably fulfill several biological functions in *A. rubens*. The current results will pave the way for our future studies that will be devoted to the clarification of the biological roles of saponins in *A. rubens* at a molecular level.

1. Introduction

Saponins form an important class of natural products first discovered in higher plants (Li et al., 2006) and then in a few marine organisms such as sea stars (asteroids) (Mackie and Turner, 1970; Kitagawa and Kobayashi, 1977), sea cucumbers (holothuroids) (Nigrelli, 1952; Yamanouchi, 1955), and sponges (Kubanek et al., 2000). Numerous studies have been conducted on these compounds that are characterized by a large chemical diversity and a wide variety of pharmacological activities (Nigrelli, 1952; Yamanouchi, 1955; Mackie and Turner, 1970; Kitagawa and Kobayashi, 1977; Kubanek et al., 2000; Li et al., 2006). Indeed, these molecules are of high interest due to their hemolytic, cytotoxic, anti-bacterial, anti-fungal, anti-viral and anti-tumor properties (Burnell and Apsimon, 1983; Hostettmann and Martson, 1995; Kalinin et al., 1995, 1996; Stonik et al., 1999; Prokof'eva et al., 2003; Maier, 2008; Jorg et al., 2011). Paradoxically their biological roles are still very speculative. Different studies have reported that saponins could be involved in several activities such as chemical defense (Mayo and Mackie, 1976; Kubanek et al., 2002; Van Dyck et al., 2011) and interspecific chemical communication (Mackie et al., 1968; Barkus, 1974; Harvey et al., 1987; Caulier, 2009). However, in all those previous studies, extracts of unresolved saponins (i.e. saponin mixtures) were used and, therefore, no data have ever been provided to associate specific saponins to the physiology or the behavior of the animal (Garneau et al., 1989). Recently, when investigating holothuroids, we separately identified saponins in the Cuvierian tubules and in the body wall of *Holothuria forskali* using mass spectrometry (MS) (Van Dyck et al., 2009, 2010a,b, 2011). Interestingly, all the saponin molecules detected in the body wall were found to be also present in the Cuvierian tubules but the latter also contain specific congeners. Furthermore, quantitative as well as qualitative differences between the saponin contents in both analyzed body parts were highlighted depending on whether the animals were subjected or not to external stress (Van Dyck et al., 2010b, 2011). All the collected data pointed to the crucial role played by several identified saponins in the chemical defense of *H. forskali*.

Unlike holothuroid saponins which are triterpenoid glycosides (Van Dyck et al., 2009), asteroid saponins are steroid glycosides (D'Auria et al., 1993; Maier, 2008). Three categories of saponins have been identified in sea stars, i.e. polyhydroxysteroids glycosides, asterosaponins and macrocyclic saponins (Kisha et al., 2001; Maier, 2008). In *Asterias rubens*,

* Corresponding authors.
E-mail addresses: Patrick.Flammang@umons.ac.be (P. Flammang), Pascal.Gerbaux@umons.ac.be (P. Gerbaux).

1096-4959/$ – see front matter © 2013 Elsevier Inc. All rights reserved.
http://dx.doi.org/10.1016/j.cbpb.2013.10.004

a common sea star living in the north-east of Atlantic Ocean, only asterosaponins have been identified (D'Auria et al., 1993). As exemplified in Scheme 1, asterosaponins are pentaglycoside or hexaglycoside sulfated steroids that have high molecular weights (±1200 Da). The aglycone moiety is a $\Delta^{9,11}$-3β, 6α-dihydroxysteroid with a sulfate group at C3 and often an oxo function at C23 on the aglycone side-chain. The carbohydrate moiety is bound at the carbon atom C6 on the aglycone and includes five to six sugar residues. The most common monosaccharides are β-D-fucopyranose, β-D-quinovopyranose, β-D-xylopyranose, β-D-galactopyranose and β-D-glucopyranose. 6-deoxy-xylo-hex-4-ulose (DXHU) and α-L-arabinopyranose are less frequently present. Numerous combinations of those chemical motifs are expected and asterosaponins are then characterized by a wide degree of structural variability. Previous researches have already identified numerous saponins from *A. rubens* (Sandvoss et al., 2000, 2001, 2003). NMR and MS techniques were extensively used to identify these molecules. In the most recent study, seventeen saponin structures were described for the animal whole body, i.e. without a previous organ separation (Scheme 1) (Sandvoss et al., 2001). These seventeen saponin congeners are characterized by twelve different compositions, exemplifying the presence of isomeric saponins.

In asteroids, it is generally considered that saponins may have a role in digestion (Garneau et al., 1989; Kisha et al., 2001), reproduction (Mackie et al., 1977; Voogt and Huiskamp, 1979; Naruse et al., 2010) and chemical signaling (Mackie et al., 1968; Thomas and Gruffydd, 1971; Mayo and Mackie, 1976; Harvey et al., 1987). In relation with these different biological functions, several studies have suggested that each organ would possess its own saponin mixture (Mackie et al., 1977; Voogt and Van Rheenen, 1982; Garneau et al., 1989; Kisha et al., 2001). However, none of these reports investigated the specific distribution of saponins in the various body components at a molecular level, i.e. by identifying the different congeners in each mixture. In the present study, we decided to use MALDI–MS and MALDI–MS/MS (Matrix-assisted Laser Desorption/Ionization Mass Spectrometry) methods to identify the saponins from *A. rubens*. Saponins from the aboral and oral body wall, the stomach, the pyloric caeca and the gonads from different individuals were extracted and analyzed separately, allowing comparisons to be made between body components and between animals. In addition, LC–MS and LC–MS/MS (Liquid Chromatography–Mass Spectrometry) methodologies were necessary to differentiate all the saponins in the extracts. This paper therefore represents a first step in the deciphering, at a molecular level, of the relationship between specific saponins and the physiology or the behavior of the animal.

2. Materials and methods

2.1. Sampling

Individuals of *A. rubens*, Linnaeus, 1758, were collected on the rocks at low tide at Audresselles (Opal Coast, France) in Winter and Spring 2012. They were transported to the Biology of Marine Organisms and Biomimetics laboratory of the University of Mons, where they were kept in a marine aquarium with closed circulation (13 °C, 33 psu). Four individuals, named 1-4 in the present report (Table 1), were rapidly dissected and their aboral body wall, oral body wall, gonads, stomach and pyloric caeca were stored separately in 90% methanol at 4 °C. In individual #3, spawning was induced by injecting 0.2 mL of a 100 μM 1-methyladenine solution in each arm and the dissection was performed after the animal had spawned (Haesaerts et al., 2005).

2.2. Extraction of saponins and purification of the extract

The body wall (oral and aboral), the gonads, the stomach and the pyloric caeca all underwent the same extraction protocol (Van Dyck et al., 2009). Each tissue was homogenized and the hydromethanolic extract was recovered after filtration under vacuum with a Buchner flask. It was then partitioned against n-hexane (v/v). The hydromethanolic phase was recovered and its water content was adjusted to 20% (v/v) then 40% (v/v), each time after the solutions were partitioned against CH_2Cl_2 and $CHCl_3$, respectively. The final hydromethanolic solution was evaporated at low pressure in a double boiler at 30 °C using a rotary evaporator (Laborota 4001 efficient, Heidolph) and dissolved in water in order to undergo chromatographic purification. The crude aqueous extract was loaded on a column packed with Amberlite XAD-4 (Sigma-Aldrich St. Louis, MO, USA). Washing the column with water removed the inorganic salts and subsequent elution with pure methanol allowed to recover the saponins. The methanolic extract was then evaporated to dryness and re-dissolved in water in order to undergo a last liquid–liquid extraction against isobutanol (v/v). The butanolic fraction which contained the purified saponins was aliquoted in Eppendorf tubes and evaporated using a Speed Vac (RC 10.22, VWR international). Once isobutanol was evaporated, the dry extract was dissolved with different volumes of water depending on the desired approximate final concentration.

2.3. Mass spectrometry

All mass spectrometry experiments were performed on two different mass spectrometers, a Waters Q-ToF Premier and a Waters Quattro Ultima in the negative ionization mode using MALDI (Matrix-assisted Laser Desorption/Ionization) ionization source and Electrospray ionization (ESI) source, respectively.

2.3.1. MALDI–ToF measurements

The MALDI source was constituted of a nitrogen laser, operating at 337 nm with a maximum output of 500 mW delivered to the sample in 4 ns pulses at 20 Hz repeating rate. All samples were prepared using a mixture of 1 mL of a 100 mg/mL solution of 2,5-dihydroxybenzoic acid (DHB) in water/acetonitrile (v/v) with 20 μL of *N,N*-dimethylaniline as the matrix (Snovida et al., 2008). The sandwich method was selected to prepare the sample/matrix co-crystal on the target plate. In this method, the sample analyte is not premixed with the matrix. A sample droplet (1 μL) is applied on top of a fast-evaporated matrix-only bed, followed by the deposition of a second layer of matrix in solvent (1 μL). The sample is then basically sandwiched between the two matrix layers. The sandwich deposit was selected to obtain a more homogeneous co-crystal surface. For the recording of the single-stage MALDI–MS spectra, the quadrupole (rf-only mode) was set to pass ions between *m/z* 250 and 1500 and all ions were transmitted into the pusher region of the Time-of-Flight analyzer where they were mass-analyzed with a 1 s integration time. For the MALDI–MS/MS experiments, the collision-induced dissociation (CID) method for ion activation was used. In those analyses, the ions of interest were mass-selected by the quadrupole mass filter. The selected ions were then submitted to collision against argon in the T-wave collision cell (pressure estimated at 0.9–1 mbar) and the laboratory frame kinetic energy (E_{lab}), typically at 80 eV, was selected to afford intense enough product ion signals. All the ions coming out of the collision cell, either the product ions or the non-dissociated precursor ions, were finally mass measured with the oa-ToF analyzer. Time-of-Flight mass analyses were performed in the reflectron mode at a resolution of about 10,000 (at *m/z* 1000). Elemental compositions of the saponin ions, see Table 2, have been determined by High Resolution Mass Spectrometry (HRMS) measurements on the MALDI-ToF instrument.

2.3.2. LC–MS measurements

For the on-line LC–MS analyses, a Waters Alliance 2695 liquid chromatography device was used. The HPLC device was coupled to the Waters Quattro Ultima mass spectrometer and consisted of a vacuum degasser, a quaternary pump and an autosampler. Sample volumes of 1 μL were injected. Chromatographic separation was performed on a non-polar column (Kinetex C18; 2.1 × 100 mm; 2.6 μm; Phenomenex) at 30 °C. The mobile phase was programmed with a constant flow

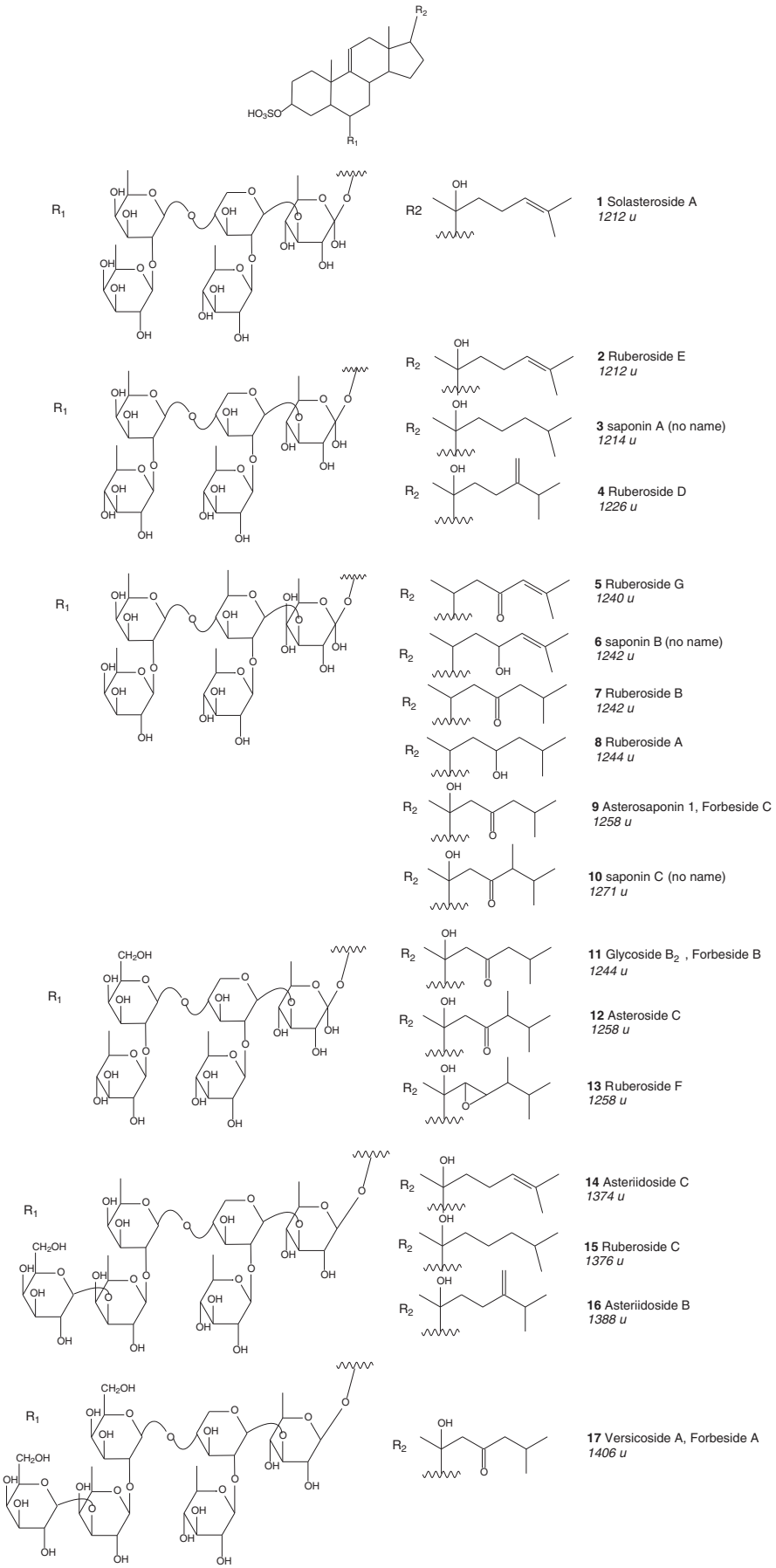

Scheme 1. Asterosaponins from *Asterias rubens* (Sandvoss et al., 2000, 2001, 2003).

Table 1
Description of the four studied individuals of *Asterias rubens*. ABW: aboral body wall; OBW: oral body wall; STO: stomach; CAE: pyloric caeca; GON: gonads.

Individual	Date of		Animal		Wet weight of the organs (g)				
#	Collection	Dissection	Weight (g)	Sex	ABW	OBW	STO	CAE	GON
1	26/01/2012	26/01/2012	158	♀	30.6	18.4	1.3	14.1	25.1
2	26/01/2012	01/02/2012	145	♂	34.7	16.4	1.1	7.9	22.1
3	12/03/2012	25/04/2012	77	♀	23.5	9.5	0.9	4.1	3.0
4	08/05/2012	11/05/2012	264	♀	71.8	22.0	2.3	27.6	31.3

(0.1 mL/min) of 20% of eluant A (water, 0.1% formic acid) and 80% of eluent B (methanol) during 15 min. The ESI conditions were: capillary voltage 3.1 kV; cone voltage 20 V; source temperature 100 °C; desolvation temperature 300 °C. Dry nitrogen was used as the ESI gas with a flow rate of 50 L/h for the gas cone and 600 L/h for the desolvation gas. The single-stage ESI–MS spectra were recorded by scanning the first quadrupole analyzer between *m/z* 250 and 1500. For the ESI–MS/MS experiments, the ions of interest were mass-selected by the first quadrupole. The selected ions were then submitted to collision against argon in the hexapole collision cell (pressure estimated at 0.9–1 mbar) and the laboratory frame kinetic energy (E_{lab}), typically at 80 eV, was selected to afford intense enough product ion signals. The product ions were finally mass measured with the second quadrupole analyzer.

2.4. Hemolytic activity

The method was adapted from Van Dyck et al. (2010a). Citrated blood from cows was used in this experiment. Erythrocytes were pelleted by centrifugation at 1000 *g* for 15 min, and were washed and centrifuged four times in cold PBS buffer (138 mM NaCl, 2.7 mM KCl, 1.5 mM KH_2PO_4, 8.1 mM Na_2HPO_4, pH 7.4) until the supernatant was clear and colorless. Two milliliters of packed cells were then diluted to 100 mL with the same buffer. Twenty microliters of each saponin extract was added to 1980 μL of the erythrocyte suspension in a microtube. The suspensions were mixed by inversion, incubated for 1 h at room temperature, and finally centrifuged (1000 *g* for 10 min). The absorbance of the clear red supernatant was then measured at 540 nm using a Labsystems multiscan MS spectrophotometer. A 10 mg/mL solution of plant saponins

Table 2
Saponin congeners detected in the different organs of *Asterias rubens* (new congeners are highlighted in gray). ABW: aboral body wall; OBW: oral body wall; STO: stomach; CAE: pyloric caeca; GON: gonads. [a]Presence in the LC–MS analysis. [b]These two saponins are enantiomers (see Scheme 1) and cannot be separated by the LC method used in this study. [c]Different names for the same structure. [d]Based on high resolution mass spectrometry measurements. [e]As exemplified in the text, the CID key losses do not involve the monosaccharide losses from the glycone part. N. D.: Not determined.

Saponin	MW (u)	$[M–H]^-$ m/z	Retention time (min)	CID key losses[e]					Composition[d]	Body distribution[a]				
				100	114	100 18	98	18		ABW	OBW	STO	CAE	GON
Solasteroside A[b]	1212	1211	7.6–8.2						$C_{56}H_{92}O_{26}S$	X	X	X		X
Ruberoside E[b]	1212	1211							$C_{56}H_{92}O_{26}S$					
Unidentified	1214	1213	5.5–6.8						$C_{56}H_{94}O_{26}S$	X	X	X	X	X
Saponin A	1214	1213	9.8–10.3						$C_{56}H_{94}O_{26}S$	X	X			X
Ruberoside D	1226	1225	9.5–11						$C_{57}H_{94}O_{26}S$	X	X			X
Regularoside B	1228	1227	5–5.5	X					$C_{56}H_{92}O_{27}S$	X	X	X	X	X
Co–ARIS III / Asterosaponin 4[c]	1228	1227	6.1–7.2						$C_{56}H_{92}O_{27}S$	X	X	X	X	X
Unidentified	1238	1237	6.1–7.6					X	$C_{57}H_{90}O_{27}S$	X	X	X		X
Ruberoside G	1240	1239	7.5–8.6					X	$C_{57}H_{92}O_{27}S$	X	X	X		X
Ruberoside B	1242	1241	6.6–6.9	X					$C_{57}H_{94}O_{27}S$	X	X			
Saponin B	1242	1241	7.4–8.9					X	$C_{57}H_{94}O_{27}S$	X	X	X	X	X
Forbeside B / Glycoside B2[c]	1244	1243	4.7–5.3	X					$C_{56}H_{92}O_{28}S$	X	X	X	X	X
Ruberoside A	1244	1243	8.1–8.6					X	$C_{57}H_{96}O_{27}S$		X			
Unidentified	1256	1255	4.3–4.7				X		$C_{57}H_{92}O_{28}S$	X	X	X	X	X
Unidentified	1256	1255	8.1–8.6	X					N. D.	X	X	X		
Forbeside C / Asterosaponin 1[c]	1258	1257	4.6–5.1			X			$C_{57}H_{94}O_{28}S$	X	X	X	X	X
Asteroside C	1258	1257	5.3–6.2		X				$C_{57}H_{94}O_{28}S$	X	X	X	X	X
Ruberoside F	1258	1257	5.8–6.9						$C_{57}H_{94}O_{28}S$	X	X	X	X	X
Unidentified	1272	1271	4.1–4.4				X	X	$C_{57}H_{92}O_{29}S$				X	X
Saponin C	1272	1271	5.3–6.2		X			X	$C_{58}H_{96}O_{28}S$	X	X	X	X	X
Unidentified	1272	1271	6.5–6.9					X	$C_{58}H_{96}O_{28}S$	X	X	X		X
Unidentified	1274	1273	4.4–5.0			X			$C_{57}H_{94}O_{29}S$	X	X	X	X	X
Asteriidoside C	1374	1373	6.9–7.4						$C_{62}H_{102}O_{31}S$	X	X	X		X
Ruberoside C	1376	1375	8.7–9.3						$C_{62}H_{104}O_{31}S$	X	X			
Asteriidoside B	1388	1387	8.4–8.8						$C_{63}H_{104}O_{31}S$	X	X			
Forbeside A / Versicoside A[c]	1406	1405	4.4–4.9	X					$C_{62}H_{102}O_{33}S$	X	X	X	X	

(from *Quillaja* bark; S 4521, Sigma-Aldrich, St. Louis, MO, USA) in PBS was serially diluted to make a standard curve (Fig. S1).

2.5. Histology

Identification of sex of the all animals was performed on the basis of a histological analysis of the gonads (Jangoux and Vloesbergh, 1973). The gonads were fixed in Bouin's fluid for 24 h and dehydrated in graded ethanol and butanol. They were then embedded in paraffin wax and sections (7 μm) were cut using a rotary microtome (Microm HM340E). The sections of the gonads were dewaxed, stained with Masson's trichrome, observed with a Zeiss AXIO Scope A1 microscope (Carl Zeiss MicroImaging, Göttingen, Germany).

3. Results and discussion

Foremost, it is important to clearly describe the different goals of the present study. The first part of this report presents the mass spectrometry approaches that we optimized to structurally characterize saponin congeners. The second part highlights the molecular diversity of saponins in different organs and different animals. In this context, we intentionally selected significantly different animals, i.e. females vs males, and collected at different moments (spring and winter). In order to even more accentuate the putative differences, we also induced spawning in one of the females with 1-methyladenine. In this context, the results of the present work cannot be used to unambiguously link saponins with biological activities, in part due to the lack of biological replicates (different animals/condition). This of course prevents assessment of the inter-individual variation, and thus hinders statistical evaluation of the data. Such investigation will represent the following part of our research, but requires the initial determination of the saponin content and the demonstration of its variability in the different organs and different animals.

3.1. Saponin diversity in A. rubens

Given the presence of a sulfate group on all the described asterosaponins from *A. rubens* (Scheme 1), the different saponin extracts were analyzed by selecting the negative ion mode, both in MALDI and ESI conditions. As a typical example, the MALDI mass spectrum of the saponin extract obtained from the oral body wall of individual #3 is presented in Fig. 1. In good agreement with the literature results (Sandvoss et al., 2000, 2001, 2003), intense signals are observed in the *m/z* 1100–1500 range and could correspond to ionized asterosaponins $[M-H]^-$. Based on the compositions of the saponin congeners listed in Scheme 1, the putative association between most of the observed ions with saponin congeners can be achieved. Indeed, the MS signals marked by a black dot on the MALDI mass spectrum are likely to correspond to the twelve compositions already identified in *A. rubens* (Scheme 1) (Sandvoss et al., 2000, 2001, 2003). For instance, the *m/z* 1243 ions — Ruberoside A **8** and/or Glycoside B_2 **11** (Forbeside B) — and the *m/z* 1257 ions — Asteroside C **12**, Ruberoside F **13** and/or Asterosaponin 1 **9** (Forbeside C) — are very abundant in the MALDI–ToF mass spectrum from the oral body wall extract of individual #3. Beside the twelve expected ion compositions, four additional signals, identified by gray dots in Fig. 1, are observed and could be associated to new saponins. For example, the signal at *m/z* 1227 could correspond to a new saponin composition never observed for *A. rubens*. It is interesting to note that this saponin possesses the same *m/z* as Co-ARIS III (Ov. Asterosaponin 4) (Scheme 2) from *Asterias amurensis* (Naruse et al., 2010).

Nevertheless, further confirmation of the presence of saponin ions is definitively required at this point of the work and evidences can only be collected by performing tandem mass spectrometry experiments on the putative saponin ions. As a typical example, the MALDI–MS/MS mass spectrum of the *m/z* 1257 ions from the oral body wall extract of individual #3 is presented in Fig. S2 and discussed in some details hereafter. Based on the compositions presented in Scheme 1, three isomeric saponins, namely Asterosaponin 1 **9**, Asteroside C **12** and Ruberoside F **13**, could account for the structure of the *m/z* 1257 ions. These three molecules differ by the side-chains attached on their aglycone moiety and by their oligosaccharide chains (see Scheme 1). Asteroside C **12** and Ruberoside F **13** possess exactly the same oligosaccharide chain.

Before starting to analyze the MS/MS data obtained on the *m/z* 1257 saponin ions and based on our previous reports on the CID behavior of saponin ions (Van Dyck et al., 2009), it is important to remind some dissociation rules that will be relevant to the present discussion. First of all, the sugar sequence in the oligosaccharide chains can be defined by following the successive losses of the monosaccharide residues from the mass-selected parent ions. Indeed, characteristic losses of 162 u, 146 u and 132 u can be associated to the presence of glucose, galactose or DXHU (162 u), of quinovose or fucose (146 u) and xylose (132 u) residues, respectively. It is also important to point out that, since the negative charge is localized on the sulfate group attached on the aglycone part, all the expected CID processes must afford fragment ions containing the aglycone moiety or part of the aglycone moiety. In other words, the description of the CID reactions must involve unwinding of the oligosaccharide chains converging to the aglycone part. Also, given the low kinetic energy regime for ion activation selected on our mass spectrometers to run the collision-induced dissociation (CID) experiments, no cross-ring cleavages of the aglycone part are expected. Nevertheless, some fragmentations involving the aglycone side-chain are likely to occur through low energy requirement reactions, such as the well-known McLafferty rearrangement. Again, based on the potential structures of the *m/z* 1257 ions, i.e. Asterosaponin 1 **9** (Forbeside C), Asteroside C **12** and Ruberoside F **13** (Scheme 1), side-chain decompositions leading to 100 u and 114 u losses are likely to occur as the first fragmentation of the mass-selected ions for, respectively, ionized Asterosaponin 1 **9** and Asteroside C **12**. Indeed, as shown in Scheme

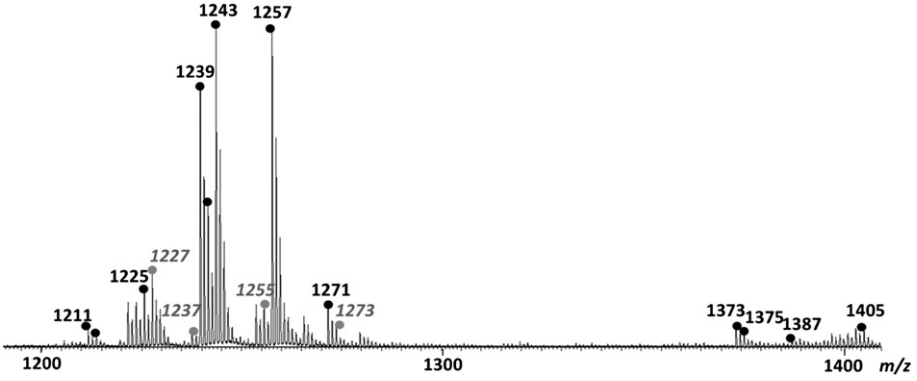

Fig. 1. Full-scan (−) MALDI mass spectrum obtained for the saponin extract from the oral body wall of *Asterias rubens* (Individual #3). MS signals marked by a black dot correspond to saponin congeners already identified in *A. rubens* while signals identified by gray dots could represent new saponins for this species (see text for details).

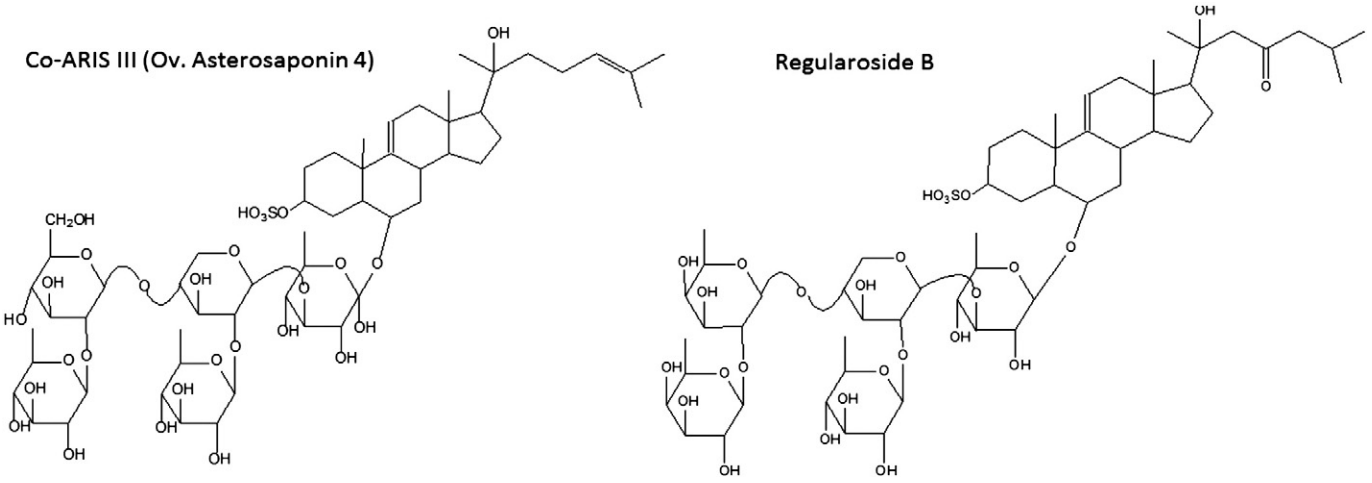

Scheme 2. Co-ARIS III (Ov. Asterosaponin 4) from *Asterias amurensis* (Naruse et al., 2010) and Regularoside B from *Culcita novaeguineae* (Tang et al., 2005) and *Coscinasterias tenuispina* (Riccio et al., 1986).

S1, McLafferty rearrangements involving 6-membered ring transition states often represent energetically and kinetically favorable processes, contrary to the glycosidic bond cleavages that are best described as a 1,2-elimination process. In the present work, a significant 18 u loss was also demonstrated to be associated with the presence of a DXHU residue in the oligosaccharidic chain (Scheme S1).

The collision-induced dissociation (CID) mass spectrum of the *m/z* 1257 ions is presented in Fig. S2. It shows the co-occurrence of four fragmentation patterns (see also Scheme 3): the two fragmentation routes represented by black lines (solid and dotted lines) can be associated to Asterosaponin 1 **9**, whereas the two other fragmentation pathways, identified by the gray lines (solid and dotted lines), are characteristic of Asteroside C **12** ions. In this spectrum, no evidence for the presence of Ruberoside F **13** can be found since no specific dissociation of the epoxide side-chain is hitherto identified. There is no evidence either for the absence of this saponin. As far as the dotted black line route is concerned, the dominant loss of 4-methylpent-1-en-2-ol (100 u — Scheme S1) as well as the occurrence of formal successive eliminations of the monosaccharide residues [fucose (Fuc), fucose (Fuc), quinovose (Qui), quinovose (Qui), 6-deoxy-xylo-hex-4-ulose (DXHU)], ultimately leading to the intense *m/z* 411 ions, unambiguously reveal the presence of Asterosaponin 1 **9** ions. The complete dissociation pathway is described in Scheme 3A. Interestingly, after the initial 100 u loss, a competitive dissociation route is also opened and is initiated by the loss of a water molecule (18 u), certainly involving the DXHU residue (Scheme S1). From the so-obtained *m/z* 1139 ions, the successive losses of the monosaccharide residues can then be detected and are highlighted by the solid black line route in Fig. S2. The DXHU origin of the expelled water molecule can be confirmed after a careful analysis of the CID mass spectrum. Indeed, when following the solid black line, i.e. *m/z* 1257 → *m/z* 1139 → *m/z* 993 → *m/z* 847 → *m/z* 701 → *m/z* 555 → *m/z* 411, it is interesting to note that the ultimate mass transition corresponds to a 144 u loss that can only be associated with the loss of a DXHU residue (162 u) that has already expelled a water molecule, see Scheme 3A. In Fig. S2, this neutral loss is identified by DXHU//. As far as Asteroside C **12** is concerned, the expected successive losses of the monosaccharide residues are clearly observed in the CID spectrum when following the solid gray line (Fig. S2). As also described in Scheme 3B, the successive losses of the monosaccharide residues correspond to the eliminations of quinovose (Qui), galactose (Gal), quinovose (Qui), xylose (Xyl) and quinovose (Qui). Based on the structure of the oligosaccharidic chain, we cannot distinguish Asteroside C **12** from Ruberoside F **13**. However, the observation of a direct 114 u loss, 3,4-dimethylpent-1-en-2-ol, from the parent *m/z* 1257 ions immediately confirms the presence of Asteroside C **12** ions (Fig. S2, dotted gray line and Scheme 3B). Inversely, no direct evidence for the presence of Ruberoside F **13** was obtained on the basis of our MALDI–MS/MS experiments.

3.2. Variability of saponin contents in A. rubens

In *A. rubens*, Voogt and Van Rheenen reported that asterosaponins are not distributed uniformly among body components and that each organ would possess its own saponin mixture (Voogt and Van Rheenen, 1982). Nevertheless, in that work, the identification of the saponin congeners within each organ was not reported. We then decided to focus on the inter-organ distribution of saponins by analyzing separately five different body components (the aboral body wall, the oral body wall, the stomach, the pyloric caeca, and the gonads) from different individuals. As already claimed, in order to get the broadest possible overview of the saponin diversity, three females and one male were sampled, with two individuals collected and sacrificed in winter time and two during spring (Table 1). Moreover, for one of the female sea stars collected during spring (individual #3), spawning was artificially induced before dissection and saponin extraction. At this stage of the work, the purpose was not to determine the biological role(s) of saponins, but we aimed to figure out their inter-organ and inter-individual variability. Saponin mixtures were analyzed qualitatively and semi-quantitatively by MALDI–MS and MALDI–MS/MS. In order to tackle the intrinsic lack of quantitative reproducibility of the MALDI analyses, we acquired sixteen MALDI mass spectra for all the extracts and reported the average relative intensity for each *m/z* ratio. It is also important to remind that the presented data correspond to relative abundance of each saponin composition (i.e. merging the isomeric saponins), not of each saponin congener. For the present analysis, we will correlate the saponin ion relative abundances to the relative molar fraction of saponin congeners within the extracts. Indeed, given the high structural similarity between the saponin congeners and based on the fact that the ionization process only involves the sulfate group (negative ion), we consider that such an approximation is reasonable. Nevertheless, to afford a more quantitative aspect to our analysis, we will also measure the hemolytic activity of the saponin extracts that is related to the concentration of saponins within the extracts.

Fig. 2 features the saponin ion distributions in each organ of the four individuals. The comparison of the average relative intensity of all the saponin ions (*m/z*) in this graph immediately confirms the heterogeneity of the saponin distribution. At first glance, it appears that saponin ions detected at *m/z* 1239, 1241, 1243 and 1257 are the most abundant molecules whatever the body component considered (see also Fig. 1).

When comparing the saponin contents of each organ between the different animals (Fig. 2), we observed that the saponin distribution in

the oral body wall (OBW) and the stomach (STO) are relatively similar; the saponins associated with the signal at *m/z* 1243 (Ruberoside A **8** and/or Glycoside B_2 **11**) being the most abundant in these two organs, closely followed by the saponins Ruberoside G **5** (*m/z* 1239) and Asterosaponin 1 **9**, Asteroside C **12** and/or Ruberoside F **13** (*m/z* 1257). Although there is some variation of the relative abundances of the saponin ions when comparing the four different animals, no clear pattern emerges. As far as the aboral body wall is concerned (Fig. 2 ABW), the

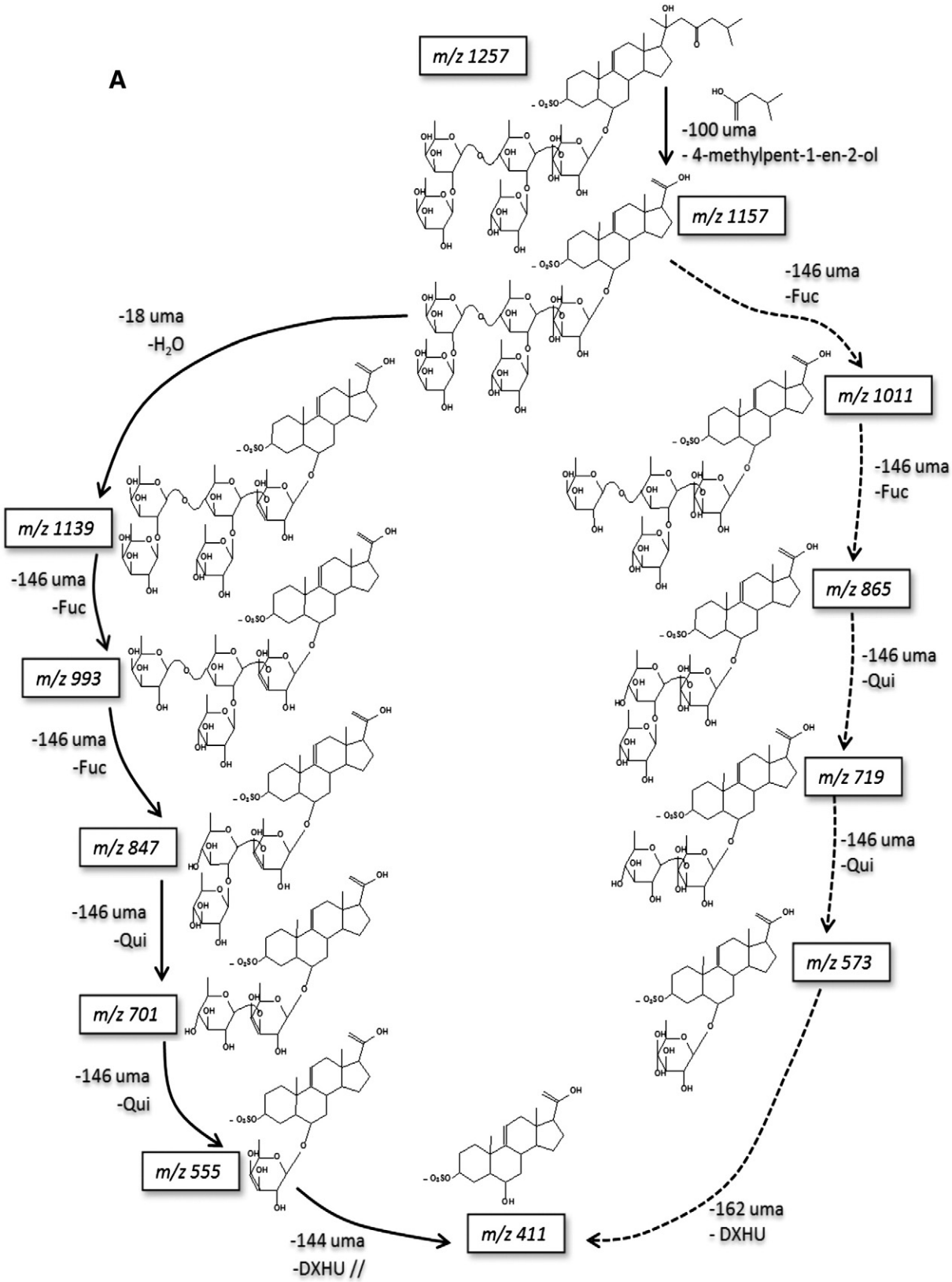

Scheme 3. Collision-induced dissociation experiments of the *m/z* 1257 ions obtained upon MALDI analysis of the oral body wall saponin extract of Individual #3: fragmentation reactions of (A) Asterosaponin 1 **9** and (B) Asteroside C **12** ions.

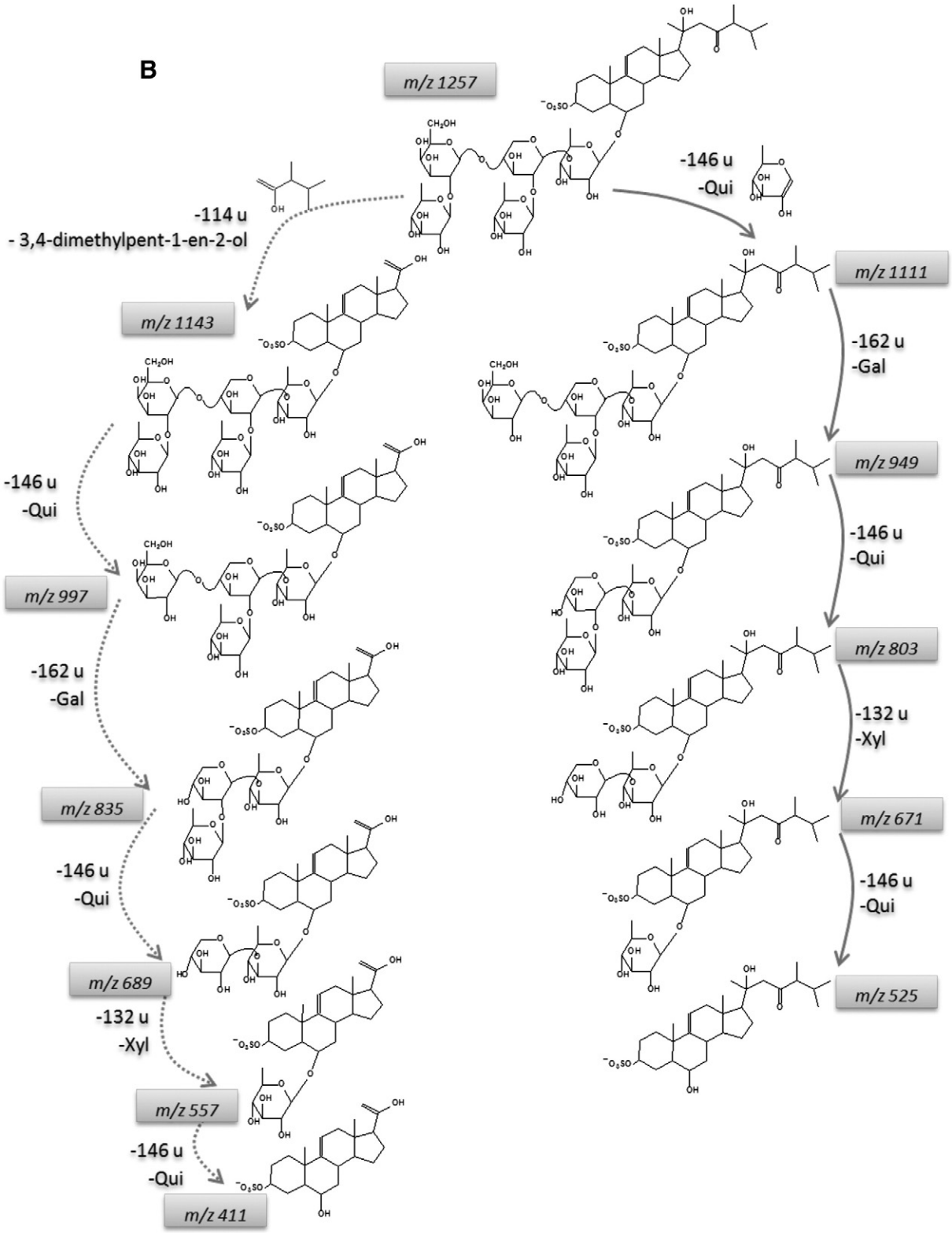

Scheme 3 (continued).

m/z 1211, 1239, 1241, 1243 and 1257 ions are the most represented saponin compositions, but significant variability is detected from one animal to the other. Interestingly, in this body component, the relative abundances of the *m/z* 1211 saponin ions (Solasteroside A **1** and/or Ruberoside E **2**) and the *m/z* 1373 saponin ions (Asteriidoside C **14**) are higher than in the other organs, whatever the animal. However, the molar fraction of the saponin molecules corresponding to the *m/z* 1211 ions decreases from individual #1 to individual #4, whereas, in the meantime, the relative intensities of the *m/z* 1243 and *m/z* 1257 ions increase. Accordingly, in the aboral body wall, the most abundant saponin ions are different from one animal to another, the *m/z* 1211 ions being the most represented in individual #1, the *m/z* 1241 ions in individuals #2 and #3, and the *m/z* 1257 ions in individual #4. The only other body compartment in which there are important inter-

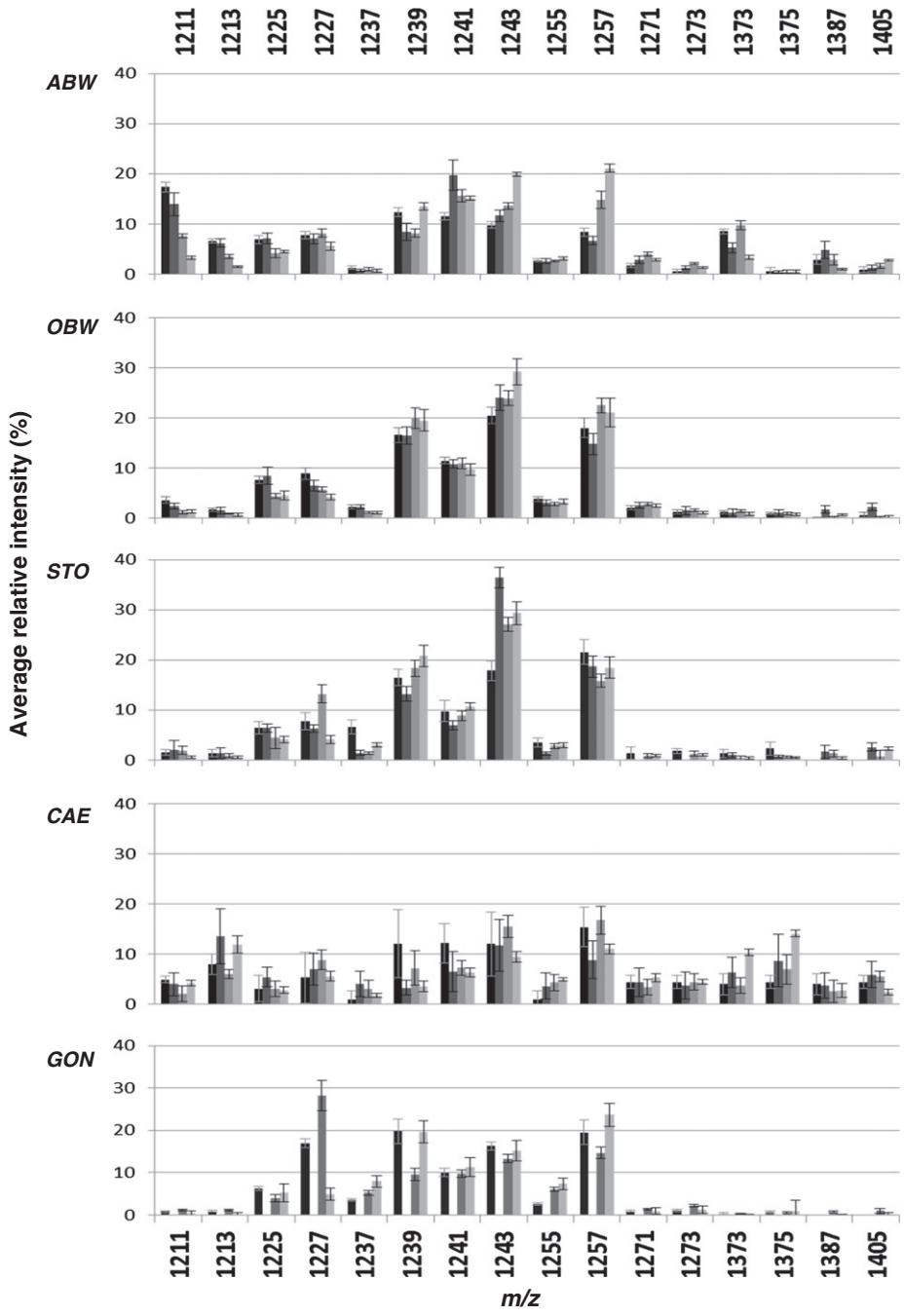

Fig. 2. Comparison of the saponin contents of the five selected organs for 4 individuals of *Asterias rubens*. The relative intensities (mean ± SD) of the saponin ions observed in the MALDI mass spectra of the extracts are used to estimate the molar fraction of the different saponins. For each extract, 16 MALDI mass spectra were recorded (see text for details). In this diagram, the saponins are only identified by their compositions and no distinction between isomeric saponins is made. ABW: aboral body wall; OBW: oral body wall; STO: stomach; CAE: pylorics caeca; GON: gonads. ■ Individual #1, ■ Individual #2, ■ Individual #3, ■ Individual #4.

individual variations in the saponin contents are the gonads (Fig. 2 GON). Only the saponin contents of the gonads from the three female sea stars are compared as no results have been obtained for the gonad extract from individual #2. Individuals #1, #3 and #4 were sacrificed in January, April and May, respectively (Table 1). The saponin contents of individuals #1 and #4 appear reasonably similar, with the saponins associated to the *m/z* 1239 and 1257 ions being the most represented saponin ions. Conversely, in individual #3, for which spawning has been induced, the saponin molecule associated with the *m/z* 1227 ions is by far the most abundant congener. Furthermore, these *m/z* 1227 ions are more intense in the gonad extracts than in the other body compartments. This molecule, which could be identified as Co-ARIS III (Ov. Asterosaponin 4) (Scheme 2), has already been identified in the egg jelly of the sea star *A. amurensis* where it has been proposed to participate to the acrosomial reaction (Naruse et al., 2010). At this level of the study, we cannot speculate on the function of the saponin molecule associated with those *m/z* 1227 ions. However, this molecule is likely to play a significant role related to spawning and/or fertilization during the reproductive period. Finally, the distribution of the saponin ions in the pyloric caeca extracts appears homogeneous, with all ions being represented (Fig. 2 CAE). However, it was quite difficult to obtain reproducible results, even when making repeated measurements on one given extract, and the large standard deviations in Fig. 2 CAE suggest that the saponin concentrations in the pyloric caeca are presumably low

compared to the other organs, generating mass spectra characterized by weak signal-to-noise ratios.

In addition to these mass spectrometry analyses, semi-quantitative data were obtained by measurement of the hemolytic activity of each saponin extract against cow blood erythrocytes (Fig. S3). These measurements clearly show that saponin concentrations vary greatly among individuals as well as among organs. Pyloric caeca are the organs presenting the lowest saponin concentrations. This is in agreement with the difficulties that we experienced to obtain reproducible results in the MALDI analyses when analyzing pyloric caeca extracts (Fig. 2 CAE). On the other hand, the highest concentrations were measured in the aboral body wall and in the gonads, although it is also in these organs that the largest differences between individuals were noted. The high saponin concentration in the gonads of the individual #3 could be linked to the induction of spawning but more data are definitely required before drawing conclusions.

3.3. LC–MS and LC–MS/MS analyses of saponins of A. rubens

At this point of the work, the results point to the high variability, both qualitatively and quantitatively, of the saponin body distribution in *A. rubens*. Nevertheless, although the developed MALDI analyses seems to be really efficient for a direct screening of saponin distribution within the organ extracts, the presence of isomeric saponins requires an additional characterization step based on a chromatographic separation prior to the mass spectrometry analyses. The presence of isomeric saponins can of course be highlighted by running MALDI–MS/MS analyses provided key-fragmentations have been previously identified for all the isomeric saponin ions. However, for some saponin ions, i.e. Ruberoside F **13**, such a fingerprint is not available.

To further validate the presence of isomers and to identify individual saponins, LC–MS and LC–MS/MS analyses were therefore conducted. In the direct continuity with the previous parts of this report, the *m/z* 1257 ions obtained from the oral body wall extract (Individual #3) were selected to illustrate the discussion. Fig. 3 shows the presence of three distinct retention times A, B and C in the *m/z* 1257 extracted ion chromatogram, indicating the co-occurrence of at least three isomers. LC–MS/MS experiments are then required to obtain further information on the saponin congeners and to connect the retention times with specific isomers. In our typical example, LC–MS/MS analyses were performed on the *m/z* 1257 ions. The corresponding LC–MS/MS spectra are gathered in the Supporting Information (Fig. S4). Basically, the MS/MS mass spectrum corresponding to the 5.06 min (A) retention time immediately confirms the presence of Asterosaponin 1 **9** since this CID spectrum is dominated by the 100 u loss. Similarly, the 114 u loss, signature of the Asteroside C **12** ions, is clearly observed in the MS/MS spectrum corresponding to the 6.11 min (B) retention time. Finally, Ruberoside F **13** is unambiguously eluted after 6.91 min

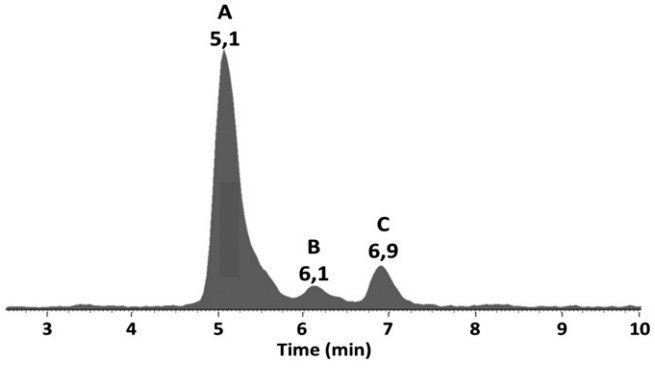

Fig. 3. LC–MS analysis of the saponin extract from the oral body wall of Individual #3: *m/z* 1257 extracted ion chromatogram.

(C) given the occurrence amongst the CID fragments of all the ions arising from the expected monosaccharide losses and the total absence of the 114 u loss.

Similar complete LC–MS and LC–MS/MS analyses have been carried out for all the saponin ions detected in MALDI–ToF mass spectrum of Fig. 1. The global results, i.e. merging all the animals, are summarized in Table 2. For all the LC–MS/MS mass spectra, the identification of the isomers was achieved (i) by measuring resolved retention times in the corresponding extracted ion chromatograms, (ii) by examining the successive monosaccharide losses (MS/MS experiments), (iii) by seeking specific losses (100, 114, 98 u) due to McLafferty rearrangement at the side chain of the aglycone and (iv) by observing the 18 u loss that was demonstrated to be characteristic of DXHU (Scheme S1). Using this method, 26 congeners were detected underlying the 16 *m/z* signals detected by MALDI–MS (Fig. 1). Nine new molecules were detected in addition to the seventeen saponin congeners already described in the literature for *A. rubens* (Table 2). Among the latter, only Solasteroside A **1** and Ruberoside E **2** (Table 2; *m/z* 1211) could not be distinguished because they are enantiomers (Scheme 1) and, as such, cannot be separated by the LC conditions used in this study. The organ distribution of all the saponins detected is presented in Table 2. Although many congeners are found in most or all organs, some saponins are restricted to one or two organs. Ruberoside A **8** detected at *m/z* 1243 is exclusively observed in the oral body wall, being therefore probably located in the tube feet. In contrast, Ruberosides B **7** and C **15**, and Asteriidoside B **16** were all specifically found in the body wall (oral and aboral). Interestingly, Ruberoside C **15** and Asteriidoside B **16** are hexaoside saponins (see Scheme 1). These congeners are presumably more hydrophilic (i.e. more soluble in seawater), suggesting they could be released in the sea water surrounding the sea stars (Van Dyck et al., 2011).

3.4. Identification of new saponin isomers

As described in the previous section, we observed on the basis of our LC–MS analyses 9 new saponin congeners that were hitherto not reported in the literature for *A. rubens*. The corresponding ions, as summarized in Table 2, are detected at *m/z* 1213 (1), 1227 (2), 1237 (1), 1255 (2), 1271 (2) and 1273 (1). The figures under brackets correspond to the numbers of different molecules for each mass-to-charge ratio. All those ions were then subjected to LC–MS/MS analyses and, based on the observed CID fragment ions (see Table 2), we tentatively propose that the two isomeric ions detected at *m/z* 1227 are respectively Regularoside B and Co-ARIS III (Asterosaponin 4), see Scheme 2. Co-ARIS III has been isolated from *A. amurensis* (Naruse et al., 2010) whereas Regularoside B was discovered in both *Culcita novaeguineae* (Tang et al., 2005) and *Coscinasterias tenuispina* (Riccio et al., 1986). The CID spectra of the *m/z* 1227 ions are presented in Fig. S5 and are clearly in agreement with the presence of ions corresponding to Regularoside B and Co-ARIS III.

Similar analyses have then been undertaken on the eight remaining saponin congeners. Based on their elemental compositions, on their CID fragmentations, on common building parts of known saponins and assuming that we are dealing with saponin ions, we gather in Table S1 some candidate molecules. Of course, further investigations are certainly required to unambiguously identify those new saponins. In the context of the present work, such a time-consuming task will be considered only if the corresponding molecules appear unambiguously to be involved in a specific biological activity.

4. Conclusions

Asterosaponins are well-known secondary metabolites of the common sea star *A. rubens* in which they would be involved in chemical defense, digestion, and reproduction. Previous studies have identified seventeen different saponin congeners in the whole individuals of this species. In the present study, we analyzed separately the saponin

content of five different organs, namely the aboral body wall, the oral body wall (including tube feet), the stomach, the pyloric caeca and the gonads. MALDI–MS, MALDI–MS/MS, LC–MS and LC–MS/MS techniques have been complementarily used and were demonstrated to be strong tools to detect these molecules in complex mixtures. MALDI techniques were used for a rapid screening of the saponin mixtures, while LC–MS techniques were used to achieve chromatographic separation of isomers. In addition to the seventeen molecules (twelve compositions) already described in the literature, nine new molecules (six compositions) have been detected. It was observed that the five different organs are each characterized by specific saponin contents. Moreover, the body wall and the gonad saponin contents varied according to the individual considered. It was also in these two organs that the highest hemolytic activity was measured, although once again large differences between individuals were noted. Finally, the body wall and the gonads are the only organs containing specific saponin congeners and, thus, they deserve more attention. In the future, the methodologies presented in this report will be used to clarify the biological roles of the saponins in *A. rubens*. Particularly, we will focus on the role played by body wall saponins in chemical defense, and on the function of gonad saponins in reproduction, at a molecular level.

Acknowledgments

The MS laboratory acknowledges the “Fonds de la Recherche Scientifique (FRS-FNRS)” for its contribution to the acquisition of the Waters QToF Premier Mass Spectrometer. P.G. and P.F. are respectively senior research associate and research director of the FRS-FNRS. M.D. and G.C. are grateful to the F.R.I.A. for financial support. This work supported in part by a FRFC research project no. T.0056.13.

Appendix A. Supplementary data

Supplementary data to this article can be found online at http://dx.doi.org/10.1016/j.cbpb.2013.10.004.

References

Barkus, G., 1974. Toxicity in Holothurians: a geographical pattern. Biotropica 6, 229–236.
Burnell, D.J., Apsimon, J.W., 1983. Echinoderm saponins. Mar. Nat. Prod. 5, 287–389.
Caulier, G., 2009. Caractérisation de kairomones impliquées dans la reconnaissance des holothuries-hôtes par le crabe symbiotique *Lissocarcinus orbicularis Dana*, 1952. Université UMONS, thèse de mémoire 1–66.
D' Auria, M.V., Minale, L., Riccio, R., 1993. Polyoxygenated steroids of marine origin. Chem. Rev. 93, 1839–1895.
Garneau, F.X., Harvey, C., Simard, S.L., Apsimon, J., Burnell, D., Himmelman, J., 1989. The distribution of asterosaponins in various body components of starfish *Leptasterias polaris*. Comp. Biochem. Physiol. B Biochem. Mol. Biol. 92, 411–416.
Haesaerts, D., Jangoux, M., Flammang, P., 2005. The attachment complex of brachiolaria larvae of the sea star *Asterias rubens* (Echinodermata): an ultrastructural and immunocytochemical study. Zoomorphology 124, 67–78.
Harvey, C., Garneau, F.-X., Himmelman, J., 1987. Chemodetection of predatory seaster *Leptasterias polaris* by whelk *Buccinum undatum*. Mar. Ecol. Prog. Ser. 40, 79–86.
Hostettmann, K., Martson, A., 1995. Chemistry & Pharmacology of Natural Products. Cambridge University Press, Saponins.
Jangoux, M., Vloesbergh, M., 1973. Contribution à l'étude du cycle annuel de reproduction d'une population d'*Asterias rubens* (Echinodermata, Asteroidea) du littoral belge. Neth. J. Sea Res. 6, 389–408.
Jorg, M.A., Vera, K., Sven, B.A., Soren, B., 2011. Molecular activities, biosynthesis and evolution of triterpenoid saponins. Phytochemistry 72, 435–457.
Kalinin, V.I., Anisimov, M.M., Prokofieva, N.G., Avilov, S.A., Afiyatullov, S.H.S.H., Stonik, V.A., 1995. Biological activities and biological role of triterpene glycosides from holothuroids. Echinoderm Studies.Balkema, Rotterdam 139–181.
Kalinin, V.I., Prokofieva, N.G., Likhatskaya, G.N., Schentsova, E.B., Agafonova, I.G., Avilov, S.A., Drozdova, O.A., 1996. Hemolytic activities of triterpene glycosides from the holothurians order dendrochirotida: some trends in the evolution of this group of toxins. Toxicon 34, 475–483.
Kisha, A.A., Ivanchina, N.V., Kalinovsky, A.I., Dmitrenok, P.S., Stonik, V.A., 2001. Sulfated steroid compounds from the starfish *Aphelasterias japonica* of the Kuril population. Comp. Biochem. Physiol. B Biochem. Mol. Biol. 128, 43–52.
Kitagawa, I., Kobayashi, M., 1977. On the structure of the major saponin from the starfish *Acanthaster planci*. Tetrahedron Lett. 10, 859–862.
Kubanek, J., Pawlik, J., Eve, T., Fenical, W., 2000. Triterpene glycosides defend the Caribbean reef sponge *Erylus formosus* from predatory fishes. Mar. Ecol. Prog. Ser. 207, 69–77.
Kubanek, J., Walen, K., Engel, S., Kelly, S., Henkel, T., Fenical, W., Pawlik, J., 2002. Multiple defensive roles for triterpene glycosides from two Caribbean sponges. Oecologia 13, 125–136.
Li, R., Zhou, Y., Wu, Z., Ding, L., 2006. ESI-Qq TOF–MS/MS and APCI–IT–MS/MS analysis of steroid saponins from the rhizomes of *Dioscorea panthaica*. J. Mass Spectrom. 41, 1–22.
Mackie, A.M., Turner, A.B., 1970. Partial characterization of biologically active steroid glycoside isolated from the starfish *Marthasterias glacialis*. Biochem. J. 117, 543–550.
Mackie, A.M., Lasker, R., Grant, P.T., 1968. Avoidance reactions of mollusc *Buccinum undatum* to saponin-like surface-active substances in extracts of thenstarfish *Astérias rubens* and *Martasterias glacialis*. Comp. Biochem. Physiol. 26, 415–428.
Mackie, A.M., Singh, H., Owen, J., 1977. Studies on the distribution, biosynthesis and function of steroidal saponins in echinoderms. Comp. Biochem. Physiol. B Biochem. Mol. Biol. 56, 9–14.
Maier, M., 2008. Biological activities of sulfated glycosides from echinoderms. Stud. Nat. Prod. Chem. 35, 311–354.
Mayo, P., Mackie, A.M., 1976. Studies of avoidance reactions in several species of predatory British seastars (Echinodermata: Asteroidea). Mar. Biol. 38, 41–49.
Naruse, M., Suetomo, H., Matsubara, T., Sato, T., Yanagawa, H., Hoshi, M., Matsumoto, M., 2010. Acrosome reaction-related steroidal saponin, Co-ARIS, from the starfish induces structural changes in microdomains. Dev. Biol. XX, 1–7.
Nigrelli, R.F., 1952. The effect of holothurin on fish, and mice with sarcoma 180. Zoologica 37, 89–90.
Prokof'eva, N., Chaikina, E., Kicha, A., Ivanchina, N., 2003. Biological activities of steroid glycosides from starfish. Comp. Biochem. Physiol. B Biochem. Mol. Biol. 134, 695–701.
Riccio, R., Iorizzi, M., Minale, L., 1986. Starfish saponins. Isolation of sixteen steroidal glycosides and three polyhydroxysteroids from the Mediterranean starfish *Coscinasterias tenuispina*. Bull. Soc. Chim. Belg. 95, 869–893.
Sandvoss, M., Huong Pham, L., Levsen, K., Preiss, A., 2000. Isolation and structural elucidation of steroid oligoglycosides from the starfish *Asterias rubens* by means of direct online LC–NMR–MS hyphenation and one- and two-dimensional NMR investigations. Eur. J. Org. Chem. 1253–1262.
Sandvoss, M., Weltring, A., Preiss, A., Levsen, K., Wuensch, G., 2001. Combination MSPD and LC–NMR–MS as a new efficient approach for rapid screening of natural products: application to the total asterosaponin fraction of the starfish *Asterias rubens*. J. Chromatogr. 917, 75–86.
Sandvoss, M., Preiss, A., Levsen, K., Weisemann, R., 2003. Two new asterosaponins from the starfish *Asterias rubens*: application of a cryogenic NMR probe head. Magn. Reson. Chem. 41, 949–954.
Snovida, S.I., Rak-Banville, J.M., Perreault, H., 2008. On the use of DHB/aniline and DHB/N, N-dimethylaniline matrices for improved detection of carbohydrates: automated identification of oligosaccharides and quantitative analysis of sialylated glycans by MALDI–TOF mass spectrometry. J. Am. Soc. Mass Spectrom. 19, 1138–1146.
Stonik, V., Kalinin, V., Avilov, S., 1999. Toxins from sea cucumbers (holothuroids): chemical structures, properties, taxonomic distribution, biosynthesis and evolution. J. Nat. Toxins 8, 235–247.
Tang, H.F., Yi, Y.H., Li, L., Sun, P., Zhang, S.Q., Zhao, Y.P., 2005. Bioactive asterosaponins from the starfish *Culcita novaeguineae*. J. Nat. Prod. 68, 337–341.
Thomas, G.E., Gruffydd, L.L.D., 1971. The types of escape reactions elicited in the scallop *Pecten maximus* by selected sea-star species. Mar. Biol. 10, 87–93.
Van Dyck, S., Gerbaux, P., Flammang, P., 2009. Elucidation of molecular diversity and body distribution of saponins in the sea cucumber *Holothuria forskali* (Echinodermata) by mass spectrometry. Comp. Biochem. Physiol. B Biochem. Mol. Biol. 152, 124–134.
Van Dyck, S., Gerbaux, P., Flammang, P., 2010a. Qualitative and quantitative saponin contents in five sea cucumbers from the Indian Ocean. Mar. Drugs 8, 173–189.
Van Dyck, S., Flammang, P., Meriaux, C., Bonnel, D., Salzet, M., Fournier, I., Wisztorski, M., 2010b. Localization of secondary metabolites in marine invertebrates: contribution of MALDI MSI for the study of saponins in cuvierian tubules of H. forskali. PLoS ONE 5, e13923–e.
Van Dyck, S., Caulier, G., Todesco, M., Gerbaux, P., Fournier, I., Wisztorski, M., Flammang, P., 2011. The triterpene glycosides of *Holothuria forskali*: usefulness and efficiency as a chemical defense mechanism against predatory fish. J. Exp. Biol. 214, 1347–1356.
Voogt, P.A., Huiskamp, R., 1979. Sex-dependence and seasonal variation of saponins in the gonads of the starfish *Asterias rubens*: their relation to reproduction. Comp. Biochem. Physiol. A Mol. Integr. Physiol. 62, 1049–1055.
Voogt, P.A., Van Rheenen, J.W.A., 1982. Carbohydrate content and composition of asterosaponins from different organs of the sea star *Asterias rubens*: relation to their haemolytic activity and implications for their biosynthesis. Comp. Biochem. Physiol. B Biochem. Mol. Biol. 72, 683–688.
Yamanouchi, T., 1955. On the poisonous substance contained in holothurians. Publ. Seto Mar. Biol. Lab. 4, 183–203.